Atmos. Chem. Phys. Discuss., doi:10.5194/acp-2017-216, 2017
Manuscript under review for journal Atmos. Chem. Phys.
Discussion started: 27 March 2017

Atmospheric Chemistry and Physics Discussions
Open Access

Sub-seasonal Variability in the Boundary Layer Sources for Transport into the Tropopause Layer in the Asian Monsoon Region

Bin Chen [1], Bärbel Vogel[2], Xiangde Xu [1] and Shuai Yang [3]

[1]State Key Laboratory of Severe Weather, Chinese Academy of Meteorological Sciences, Beijing 100081, China

[2]Forschungszentrum Jülich, Institute of Energy and Climate Research – Stratosphere (IEK-7), Jülich, Germany

[3]Institute of Atmospheric Physics, Chinese Academy of Sciences, Beijing 100029, China

Correspondence to: Bin Chen (chenbin@camscma.cn)

Abstract. The Asian summer monsoon (ASM) is associated with an upper-level anticyclone and acts as a well-recognized conduit for troposphere-to-stratosphere transport. The Lagrangian dispersion and transport model FLEXPART forced by ERA-Interim data from 2001-2013 was used to perform climatological modeling of the summer season (May-July). This study examines the properties of the air mass transport from the atmospheric boundary layer (BL) to the tropopause layer (TL), with particular focus on the sub-seasonal variability in the tracer-independent BL sources and the potential controlling mechanisms. The results show that, climatologically, the three most impactful BL source regions are northern India, the Tibetan Plateau, and the southern slope of the Himalayas. These regions are consistent with the locations of sources identified in previous studies. However, upon closer inspection, the different source regions to the BL-to-TL air mass transport are not constant in location or shape and are strongly affected by sub-seasonal variability. The contributions from the Tibetan Plateau are most significant in early May but decrease slightly in mid-May to mid-June. In contrast, the contributions from India and the southern slope of the Himalayas increase dramatically, with peak values occurring in mid-July. Empirical Orthogonal Function (EOF) analysis provides further evidence that the BL sources in the ASM region vary across a wide range of spatiotemporal scales. The sub-seasonal behavior of these BL sources is closely related to the strength of persistent deep convection activity over the northern Bay of Bengal and its neighboring areas.

Atmos. Chem. Phys. Discuss., doi:10.5194/acp-2017-216, 2017
Manuscript under review for journal Atmos. Chem. Phys.
Discussion started: 27 March 2017

1 Introduction

During the boreal summer, the off-equatorial Asian monsoon circulation in the upper troposphere and lower stratosphere (UTLS) features a unique persistent anticyclone, referred to as the Asian summer monsoon (ASM) anticyclone or South Asia high. The ASM anticyclone is associated with a region in which surface emissions have been shown to enter the lower stratosphere in the Northern Hemisphere (e.g., Bannister et al., 2004; Fu et al., 2006; Randel and Park, 2006; Park et al., 2009;Randel et al., 2010; Wright et al., 2011; Vogel et al., 2014; Vogel et al., 2015; Müller et al., 2016).

Because Southeast Asia and its neighboring regions are characterized by increasing surface emissions and the densest population in the world, both the anthropogenic pollutants and other radiative active species such as water vapor emitted from these regions may be transported into the Northern lower stratosphere, thereby strongly affecting the radiative forcing associated with global climate change (Forster and Shine, 1997;Hegglin et al., 2010;Solomon et al., 2010;Scheeren et al., 2003;Deng et al., 2008;Vogel et al., 2014). Satellite data have provided evidence of a pronounced chemical signature associated with enhanced troposphere-sourced trace gas species and other pollution and burned biomass tracers in the ASM anticyclone in the UTLS (Randel and Park, 2006;Park et al., 2008;Randel et al., 2010;Bian et al., 2012). In this context, meteorologists have recently begun to pay considerable attention to the transport processes for atmospheric transport from the boundary layer (BL) to the tropopause layer (TL) in the vicinity of the anticyclone and the associated underlying mechanisms (e.g., Li et al., 2005;Park et al., 2008;Gettelman et al., 2011;Rauthe-Schöch et al., 2016;Müller et al., 2016;Randel et al., 2016; Pan et al., 2016).

Although considerable efforts have been made to explore these issues, the properties of the BL-to-TL transport over the ASM region remain unclear. In particular, as a fundamental property of the transport process, the primary BL source regions and their relative degrees of importance have long been debated (Fu et al., 2006;Wright et al., 2011;Bergman et al., 2013;Orbe et al., 2015;Yan and Bian, 2015;Garny and Randel, 2016;Pan et al., 2016;Chen et al., 2012;Heath and Fuelberg, 2014).

In general, the previous studies related to BL source identification in the ASM region can be roughly divided into two categories: tracer-independent Lagrangian trajectory analysis and chemical tracer-based numerical analysis. As Lagrangian analysis studies, Fu et al. (2006), Wright et al. (2011), and Heath and Fuelberg (2014) emphasized the regions of the Tibetan Plateau (TP) and the southern slope of the Himalayas as the most important BL sources transporting air into the lower stratosphere. Based on a perspective of the whole ASM region, Chen et al. (2012) found that the Tibetan Plateau is less important than the western Pacific as a source region for tracers in the TL. Bergman et al. (2013) found that air masses originating from the Tibetan Plateau and India/SE Asia are the most important. Above mentioned efforts were made with different periods, different mean vales or with different criteria for the region of the Asian monsoon anticyclone (e.g., pressure level, potential temperature, different latitude-longitude regions). It is therefore difficult to directly compare the different results.

In addition to trajectory analysis, numerous studies have utilized carbon monoxide (CO) as a tracer to identify the BL sources. For example, Park et al. (2009) showed that the main surface sources of CO in the ASM anticyclone are India and Southeast Asia and that the contributions from the Tibetan Plateau are weak due to the lack of significant surface emissions in this region in their model simulations. Yan et al. (2015) further demonstrated that the CO within the anticyclone mostly comes from India and that little comes from East China. More recently, Pan et al. (2016) stated that the boundary layer air is primarily uplifted along the southern edge of the Tibetan Plateau and the region including northern India, Nepal and Southwestern China.

As it stands, most previous studies are restricted to case studies or relatively short time periods and do not evaluate the spatiotemporal evolution of BL sources in sufficient detail. The ASM anticyclone is not static; instead, it oscillates in strength,

Atmos. Chem. Phys. Discuss., doi:10.5194/acp-2017-216, 2017
Manuscript under review for journal Atmos. Chem. Phys.
Discussion started: 27 March 2017

shape and position throughout the summer monsoon season (Zhang et al., 2002; Vogel et al., 2015; Nützel et al., 2016;). Recently, Vogel et al. (2015) found that the contribution of different boundary source regions to the ASH strongly depends on its sub-seasonal variability and is therefore more complex than previously believed. Pan et al. (2016) further highlighted that the sub-seasonal dynamics of the ASM anticyclone are an important driver of UTLS chemical transport. The results of these studies based on chemical tracers depend heavily on the distribution of the tracer sources (Park et al.,2009). For instance, due to the lack of surface emissions, the contributions from certain sources regions, such as the Tibetan Plateau and the southern slope of the Himalayas, are likely seriously underestimated. Therefore, a tracer-independent evaluation of the sub-seasonal variability in BL sources and the associated controlling mechanisms is crucial for improving our understanding of the distribution and variation in the chemical composition of the ASM anticyclone in the UTLS.

Therefore, we use the day-to-day BL source locations identified from the BL-to-TL transport to examine the spatiotemporal evolution of convection sources at the sub-seasonal scale in this study. This study therefore focuses on the following questions in particular:

1. From which geographical region does the air reaching the TL over the ASM region originate, particularly from a climatological perspective?
2. What are the main features of the sub-seasonal variability in these BL sources?
3. Are the sub-seasonal variability and the atmospheric thermal or dynamical situations closely related?

To answer these questions, we performed multi-year Lagrangian simulations using the three-dimensional transport and dispersion model FLEXPART (Stohl et al., 2005) and summertime (May-Aug) ERA-Interim data (Dee et al., 2011) from the European Centre for Medium-Range Weather Forecasts (ECMWF) for 2000-2013. By applying

Atmos. Chem. Phys. Discuss., doi:10.5194/acp-2017-216, 2017
Manuscript under review for journal Atmos. Chem. Phys.
Discussion started: 27 March 2017

a 3D labeling technique to the kinematic trajectories, a large ensemble of selected BL-to-TL trajectories (defined as those leaving the BL and reaching the TL during their transport) was built, allowing us to conduct a tracer-independent evaluation of the primary BL-departing source regions. The analysis of 6-hourly BL source distributions is used to explore the sub-seasonal variability and associated mechanisms.

The remainder of this paper is organized as follows. Section 2 details the data, trajectory model setup, and methods used to identify the BL source regions. Section 3 presents the main results, including the climatologic state of the geographic sources, the sub-seasonal variability, and the possible association with the atmospheric conditions, followed by a conclusions and some remarks in Section 4.

2 Data, model, and methodology

2.1 Trajectory model and its configuration

Lagrangian dispersion and transport models that track large numbers of air parcel trajectories are well suited for exploring the transport of trace substances, air mass sources and sinks, and the influence of transport on the atmospheric composition of the UTLS (Berthet et al., 2007;James et al., 2008;Hoor et al., 2010;Orbe et al., 2015;Vogel et al., 2016). This study uses the 3D Lagrangian particle transport and dispersion model FLEXPART. This robust model was originally designed to calculate the long-range and mesoscale dispersion of point source-generated air pollutants, such as those emitted by a nuclear power plant accident (Stohl and Seibert, 1998; 2005). The model calculates the trajectories of so-called tracer particles using the mean winds interpolated from analysis fields and parameterizations representing turbulence and convective transport (Forster et al., 2007). These small-scale processes, which are not included in standard trajectory models, are important for realistically simulating trace substance transport (Stohl et al., 2005). The inclusion of these factors makes the calculations more computationally demanding and the statistical analysis of the model results more complex. In general, the FLEXPART model accurately simulates long-range mesoscale transport, diffusion, and the radioactive decay of the released tracers (Stohl et al., 2005).

Similar to our previous work (e.g., Chen et al., 2012a; 2017), a "domain-filling" method is used for the initialization of the FLEXPART model. The majority of the atmospheric column above the ASM region (0°N–60°N and 0°E–160°E) is divided into 2.2 million homogeneous air parcels, each representing an equal mass (approximately 1.12×10^{12} kg) with annual changes in the total atmospheric mass. The period of simulation is from 00:00 UTC April 15 to 00:00 UTC August 31 for each year; however, the analyses are based on the model output for May 1 to July 31. The FLEXPART model output, including the particle ID numbers, 3D spatial positions (i.e., latitude, longitude, and height above ground), and other physical interpolated meteorological parameters (temperature, specific humidity, air density, atmospheric BL height and the tropopause height at the position of the particle) were recorded at 6-hour intervals (03, 09, 15 and 21 UTC).

2.2 Data

The FLEXPART model can be controlled by meteorological input data generated by a variety of global and regional models. Here, ERA-Interim reanalysis data (Dee et al., 2011) from the European Centre for Medium-Range Weather Forecasts (ECMWF) are used as meteorological field inputs to feed the FLEXPART model. The ERA-Interim includes a 4D variation assimilation system and produces a grid resolution of 0.75º × 0.75º longitude/latitude at 6-hr intervals (00, 06, 12 and 18 UTC), with 60 vertical levels from the ground to 0.1 hPa.

Additionally, to represent the strength of convection activity, daily outgoing longwave radiation (OLR) at a 2.5° × 2.5° horizontal resolution during 2001-2013 derived from the National Oceanic and Atmospheric Administration (NOAA) polar-orbiting satellites (Liebmann, 1996) is used as a proxy for convection.

2.3 BL source identification

This study pays special attention to air mass transport from the atmospheric planetary BL to the TL over ASM anticyclone regions (0°N–50°N and 20°E–160°E). A Lagrangian approach is adopted to identify BL-to-TL events. Thus, the sub-ensemble BL-to-TL trajectories are selected and rigorously defined as those trajectories with altitudes below the BL height at any time step that then cross the tropopause within the ASM anticyclone during their forward tracking during the period from May 1 to August 31. The BL heights are calculated by the model using the critical Richardson number concept following the approach of Vogelezang and Holtslag (1996). The tropopause in this study is a combination of the dynamical (2PVU) and thermal tropopause (Stohl et al., 2005). Additionally, to filter out "transient" transport events, we apply a residence time criterion to the transport trajectory selection (Wernli and Bourqui, 2002). This criterion requires a trajectory to remain within the stratosphere for at least 24 h after crossing the tropopause. Thus, only "significant" BL-to-TL trajectories are taken into account.

Similar to the approach adopted in previous studies (Berthet et al., 2007; Chen et al., 2012), the selected BL-to-TL trajectory ensembles are used to identify the source regions for air transport from the BL to the TL within the ASM anticyclone and neighboring regions. The BL source locations are back-calculated from the first encounter of a BL-to-TL trajectory with the planetary BL. Building on these large ensemble data, we can create a well-resolved density field by aggregating all the trajectories into the appropriate longitude-latitude "bin" and can then investigate the relative importance of different geographical regions as sources of BL air in the TL and their spatial and temporal distribution on a regional scale. As stated in Berthet et al. (2007), the BL-to-TL trajectories accurately represent the BL-to-TL air mass transport during the simulation period and act as a measure of the "density" of particles leaving the BL. Thus, this information can be used to quantitatively compare the relative importance values of different source regions.

Atmos. Chem. Phys. Discuss., doi:10.5194/acp-2017-216, 2017
Manuscript under review for journal Atmos. Chem. Phys.
Discussion started: 27 March 2017

2.4 Statistic analysis methods

Empirical Orthogonal Function (EOF) analysis is used here to quantitatively investigate the variability in the spatial-temporal patterns of BL sources. In this study, the daily BL source data were used to examine the spatial-temporal variability. Because the BL sources vary obviously over southeastern Asian and its neighboring regions (as shown in Fig. 1), we highlighted the BL source patterns prior to calculating the EOFs. First, to eliminate the effects of noise resulting from the less important regions, only regions with variance values larger than 1.0 (Fig. 1b) were considered here. Additionally, BL sources anomalies were computed by subtracting the May-June-July means from the total field at each grid point for each year. We examined the three leading EOFs and used their associated principal components (PCs) to identify when large-amplitude patterns in the BL sources and other variables.

A number of steps are required to form composites analysis. This study selected the top 50 values of high and low PCs to assign selected events. Specifically, the atmospheric conditions of 50 days with high PCs are compared with those of 50 days with low PCs. After the high and low values are chosen, their corresponding atmospheric dynamical and thermal conditions, including wind fields at 850 hPa, convective available potential energy (CAPE) and OLR, are averaged. The low values are subtracted from the average of the high values to form the composite. Finally, the statistical significance is determined using a two-tailed Student's t-test.

In addition, wavelet transform can be used to effectively extract hidden frequency-based information from the raw signal, which is normally present in the time domain. Here, Morlet wavelet analysis is used to analyze the source variability for certain target regions. The mathematical steps, algorithms and software packages have been thoroughly described and are readily available, making this an easy-to-use technique for climate data analysis.

3 Results and discussion

3.1 Climatological features of BL sources

3.1.1 Summer seasonal mean

To provide a climatological perspective of the BL sources, we first present the summer mean of BL sources over the ASM region prior to analyzing the sub-seasonal variability. The averaged density fields for all the BL-to-TL trajectories in the BL in the 1º×1º longitude-latitude bin for the summer season (MJJ) for 2000-2013 are presented in Fig. 2. As mentioned in Section 2, the density field shows the BL source distribution and the relative importance of different geographical regions as sources for BL-to-TL transport. Climatologically, the source regions include vast regions of southern Asia, central-east China, the western Pacific, and even eastern Africa. However, as expected, the most influential sources, i.e., those with larger values, are concentrated in regions with strong convective activity: India and its northern areas, the Tibetan Plateau, and the northern Indochinese Peninsula. This distribution pattern does not match those of previous studies that used CO as a chemical tracer (Park et al., 2009;Vogel et al., 2015;Yan and Bian, 2015; Pan et al., 2016).

The seasonal BL sources presented here are largely consistent with those that have been found in previous tracer-independent studies by Wright et al. (2011) and Bergman et al. (2013), both of which identified the Tibetan Plateau and southern Asia, as well as their neighboring regions, as source regions. A closer look also reveals that the BL sources identified here differ from some previous studies based on trajectories analysis. For example, Fu et al. (2006) and Heath et al. (2014) stressed the importance of the Tibetan Plateau and the southern slope of the Himalayas, whereas Vogel et al. (2015) argued that the contributing sources are primarily located in Southeast Asia, India, and eastern and southern China. However, these studies are limited to short time periods or are case studies, which may hinder the ability to draw more general conclusions. Here the inter-annual variability is taken into account to draw more general conclusions from a climatological perspective.

The western Pacific also acts as a BL source but is less important than previously described in our earlier study (Chen et al., 2012). Obvious differences are present between our two analyses: the present analysis was restricted to BL-to-TL trajectories mostly within the ASM anticyclone, whereas the previous analysis focused on the entire ASM region. Additionally, the analysis here utilized the ECMWF interim analysis, whereas the previous study was based on the NCEP/GFS analysis. The differences in vertical velocity between these two data sets might give rise to the discrepancies between the two analyses, but further analysis of the mechanisms is beyond the scope of this study. Compared to the previous studies restricted to shorter time periods, the 13-year climatologic BL source distribution (Fig. 2) provides a better quantitative description of the geographic source regions associated with the transport of BL air mass to the UTLS in the ASM region, which presumably influences the chemical nature of the atmosphere in this region.

3.1.2 Variance and coefficient of variation

The coefficient of variation (CV) and variance for the BL-to-TL sources are calculated from the daily time series for each grid cell and are shown in Fig. 1. Because the CV is a measure of the dispersion of data points in a data series around the mean, small values are associated with source regions with little variability in their contributions, whereas large values are associated with regions that are only infrequently sources. The most impactful BL-to-TL source regions have CV values of less than 3.0 (Fig. 2) and are also characterized by large variance values (Fig. 1b), indicating marked variability. Based on Figs. 2a and 2b, the most influential BL source regions of large uplift identified in this study are the Indian peninsula, northern India, the Tibetan Plateau and the northern Bay of Bengal. These areas not only contribute significantly to the BL-to-TL transport during the summer season but also feature distinctive sub-seasonal variability.

Atmos. Chem. Phys. Discuss., doi:10.5194/acp-2017-216, 2017
Manuscript under review for journal Atmos. Chem. Phys.
Discussion started: 27 March 2017

Atmospheric Chemistry and Physics Discussions

3.1.3 Time series for air mass transport

To provide a quantitative overview, the daily evolution of BL-to-TL uplift for each year from 2000-2013 is calculated by counting the number of tropopause-crossing trajectories and multiplying this number by the mass of the air parcels. Analysis of the geographic source contributions in individual years reveals slight differences among different years, as shown in Fig. 3a. This annual variability is presumably associated with the annual variations in the strength of the ASM. The multi-year average time series (Fig. 3b) shows that the air mass transport tends to increase from May 1 to July 31, in agreement with the ASM trend (Ding, et al., 2005). The times series for each individual year suggests that the BL-to-TL sources feature significant sub-seasonal variability, highlighting the role that variability in atmospheric conditions plays in the transport of chemical tracers from the BL to the TL (Pan et al., 2016;Li et al., 2016). This sub-seasonal variability in BL sources and the relationship between the BL sources and the atmospheric conditions are explored further in Sections 3.2 and 3.3, respectively.

3.2 Sub-seasonal variability

3.2.1 Monthly mean

The multi-year averaged density fields of all the BL-to-TL trajectories within the BL for different months (May, June and July) are presented in Fig. 4. Not surprisingly, the areas with large monthly mean values for May, June and July partly overlap, particularly in the regions that have been identified as the most significant areas, i.e., northern India, the Tibetan Plateau, and Southeast Asia. However, Fig. 4 also shows an obvious shift in the BL source regions from May to July. The greatest "hotspot" for BL-to-TL transport in May is located in southern India, followed by the Tibetan Plateau and adjacent regions. These hotspots tend to become more significant in June. The sources in southern India shift northward (Vogel et al., 2015), extending to northern India and the southern slope of the Himalayas. The contributions of the Tibetan Plateau and other “hotspots” also tend to increase. In July, most of India continues to act as the most obvious "hotspot", but the area of this "hotspot" has decreased dramatically. The sources centered on northern India and the southern slope of the Himalayas have become influential, while the source centered on southern India has become insignificant. Additionally, the contribution of the western Pacific source to the BL-to-TL air mass transport has also strengthened and covers a wider area in July. In July, the Tibetan Plateau turns into a BL source region with a considerable contribution.

3.2.2 Regional contribution

To estimate the relative role of specific regions within the ASM area and to rigorously quantify the sub-seasonal variation in the BL sources, five main source regions are usually compared: the Tibetan Plateau (TP, elevations greater than 2.5 km), India and its north regions (IN, continent), southeastern China and the Indochinese Peninsula (SC, continent), the Bay of Bengal and Arabian Sea (BB, ocean), and the western Pacific (WP, ocean). The five areas are shown in Fig. 5. Based on a multi-year analysis of a daily data set, we calculated the regional contributions of the five areas to the BL-to-TL transport. Fig. 6 presents the temporal evolution of integrated net masses of the air masses uplifted from the BL and the relative contributions of the five regions during the summer season (MJJ).

The IN region almost maintains its status as the dominant source throughout the whole summer season, with a maximum relative contribution of approximately 40% in June (almost 2 times greater than the second highest contributor, SC). The amount of air mass uplift started to increase dramatically at the beginning of May, reached a peak value of approximately 4.1×10^{14} kg in mid-June, then decreased slightly. The largest relative contribution value in the IN region appears earlier than that of the net uplift for the entire source region. Therefore, compared to the other four sectors, the IN region, located the farthest of south, responds early and considerably to the progression of the ASM.

The evolution of the TP contribution is complex and interesting. Notably, the TP acts as the greatest contributor in early May, supplying 2.1×10^{13} kg (more than IN, with approximately 1.6×10^{13} kg). A large number of studies have shown that high elevations combined with intense surface heating leads to warming of the air column over the TP and very high BLs, especially in the semiarid western part of the Tibetan Plateau, before the onset of the Asian monsoon (Sugimoto and Ueno, 2010;Yanai and Li, 1994). This warming lifts the BL air masses in this region across the tropopause. Thus, the large contribution from the TP source in early May could be due to the strong sensible heating before the onset of the ASM (Wu and Zhang, 1998). However, the air mass lifting over the TP quickly decreases dramatically toward the beginning of June. This decrease presumably coincides with the decrease in sensible heating in this region. As the summer monsoon progresses (He et al., 2007), the deep convection activity in this region becomes stronger, leading to the transport of more air masses to the TL (Bergman et al., 2013;Fu et al., 2006). In this sense, the occurrence of a steady and slight increase in the relative contribution from early June to mid-July can be regarded as a response to the strengthened uplift driven by the strong convection activity associated with the advance of the ASM. In mid-July, the rain belt reaches the Tibetan Plateau, and convection is suppressed, weakening the convection over the TP region and resulting in less air mass uplift.

The continental SC region appears to be a steady contributor during the summer season, supplying 1.5×10^{14} kg. Its relative contribution (approximately 10%) remains almost unchanged. The contributions of the oceanic WP region are nearly the same as those of the IN region (5%–10%). However, obvious differences exist in the sub-seasonal variability characteristics of the oceanic regions. The contributions from the WP increase slightly at the beginning of June after an early decrease. In contrast, the contributions of the BB rise in the middle of June followed by a decrease. Their variation patterns appear to be out of phase, possibly due to the progression of the summer monsoon and variability in sea surface temperatures. However, the multi-year mean might affect the reliability of these findings, and the underlying mechanism requires further study, which is beyond the scope of this study.

The concentrations of chemicals in the UTLS at a given time can be regarded in part as the "fingerprint" of BL-to-TL transport by wind or vertical air currents (Vogel et al., 2014). Thus, the sub-seasonal variations in the BL sources, which exert substantial impacts on the BL-to-TL air mass transport over the ASM region during the summer, modulate the distribution of chemical components and concentrations in the UTLS over the ASM region. Overall, the results presented here differ from the conclusions of previous studies. For instance, the source regions are generally accepted to be the chronic deep convective regions over the South China Sea and the Bay of Bengal (Randel et al., 2016). To some extent, these discrepancies result from the analysis of short time periods or the failure to consider sub-seasonal variability in previous studies. In addition, the low level of pollutant emissions (e.g., CO) in certain regions led to inappropriate conclusions in previous chemical model-based analyses. For example, the Tibet Plateau acts as a significant BL source but is not detected in studies based on CO simulation analysis (Pan et al., 2016;Yan and Bian, 2015).

3.2.3 Sub-seasonal fluctuation

Previous studies have noted that the intraseasonal oscillations at so-called sub-6–25-day (Vincent et al., 1998) and 30–60-day (Madden and Julian, 1994) time scales strongly control the convection activity over the ASM region during the summer monsoon. Studies have reported that both 10–24-day and 30–60-day intraseasonal oscillations in convection tend to fluctuate out of phase among different regions from May to August (Chen et al., 2000).

The two boxed regions shown in Fig. 2, representing portions of the TP (25°–35°N, 85°–95°E) and IN (15°–25°N, 75°–85°E), have been selected to examine the sub-seasonal-scale BL source fluctuations over the TP and IN, respectively. We applied Morlet wavelet analysis to the time series of daily area-averaged BL sources

Atmos. Chem. Phys. Discuss., doi:10.5194/acp-2017-216, 2017
Manuscript under review for journal Atmos. Chem. Phys.
Discussion started: 27 March 2017

derived from these two key regions for 2000-2013. In addition to the apparent approximately 90-day oscillation inducing interannual variation in the ASM, the TP source anomaly wavelet spectrum shows two statistically significant peaks (at the 90% significance level) with periods of approximately 10–20 days and 30-60 days during the MJJ period (Fig. 7). The IN anomalies also exhibit marked sub-seasonal variation but to a lesser degree over a period of 10–20 days compared to the TP anomalies. This result indicates that the convection activity over the TP and IN regions exhibits substantial sub-seasonal variability during the summer. Distinct 10-20-day and 30–60-day low-frequency oscillations exist in both of these key regions from May to July.

3.3 Relationship between sub-seasonal variability and atmospheric conditions

3.3.1 Spatial pattern of sub-seasonal variability: EOF analysis

The above analysis demonstrates that the surface sources of BL-to-TL transport during the summer season exhibit sub-seasonal variability. However, the possible controlling mechanism and the relationship between sub-seasonal variability and variations in the atmospheric dynamical and thermal structure remain unclear. In this section, we examine these issues through spatiotemporal statistical analysis using EOFs and composite methods.

The three leading EOFs are shown in Fig. 8, together with the corresponding time indexes. The three leading EOFs exhibit broad spatial patterns and explain more than 37.1% of the variability. Recall that the EOFs are computed using anomaly values of the daily BL source data; thus, they are better able to depict the patterns of BL source variability. The sources in the dominant pattern (EOF1), which explains 14.6% of the variance, exhibit a south-north dipole. Obviously positive values are mainly located in the northern Bay of Bengal, the middle of India and the Indochinese Peninsula. Contrasting to the positive values, negative values cover a wide range of areas, including the southeastern Tibetan Plateau, southeastern China, and the southern slope of the Himalayas. The regions of negative values agree well with the main sources identified by Bergman et al. (2013) and Pan et al. (2016). The second EOF pattern, EOF2, accounts for 12.7% of the variance and features a negative region over India and the southern slope of the Himalayas and a smaller negative region over the Tibetan Plateau. Like EOF1, EOFs, which explains 9.8% of the variance, also features a zonal dipole pattern. Positive PC3 values are associated with the potential for strong BL source anomalies centered over the southeastern Tibetan Plateau and its adjacent regions, whereas negative PC3 values are associated with BL source anomalies over the eastern Tibetan Plateau, India and the Indochinese Peninsula. Large maximum and minimum values are associated with distinct regions with strong sub-seasonal variability.

Notably, although the EOFs maximize the explained variance over the entire domain, this analysis might result in nonphysical patterns (Alexander et al, 2015). Thus, all spatial patterns and PCs obtained from the EOF analysis should not be assumed to fully describe variations in the associated phenomena (Roundy et al., 2015). However, this observation does not deter us from making some inferences based on the EOF patterns. For example, EOF1 mainly reflects the seasonal advance of the Asian summer monsoon and represents the greatest contribution to the sub-seasonal variability in the sources. This finding is supported by the corresponding PC1, which mainly shows seasonal variability. EOF2 and lower-order EOFs/PCs show the importance of the strong uplift over India and the southern slope of the Himalayas. Therefore, the EOF analysis further documents the intra-seasonal evolution of the BL sources and demonstrates that the ASM circulation is an important element in regulating the relative importance of different sources.

3.3.2 Relationship between sub-seasonal variability and atmospheric conditions: composites analysis

To better understand the mechanisms controlling the sub-seasonal variability, we examine the synoptic composites based on the largest-amplitude values of the three leading EOFs. The top 50 negative and positive values of the PCs were selected to construct composites of low-level wind fields at 850 hPa, CAPE and OLR. We hypothesized that the discrepancy between the atmospheric conditions associated with high PC values and those associated with low PC values explains the controlling mechanisms to some extent.

The high PC1 value composite and the differences between this composite and the low value composite are shown in Fig. 9. For the high PC1 values, the atmospheric circulation is characterized by obvious zonal transport. However, for the low PC1 values, enhanced southwest circulation occurred in the lower levels over the Arabian Sea, India, the Bay of Bengal, the southeastern coast of China, and northeastern Korea (Fig. 9b). There are two enhanced regions of CAPE, one along the edge of the Arabian Sea and the other over the Bay of Bengal at approximately 10-20ºN (Fig. 9d). The deep convection (represented by OLR) anomalies are centered on India and extend from the low-latitude oceanic areas to inland areas, forming a southwest-oriented belt. These areas of enhanced convection are consistent with the major transport pathways associated with the southeast summer monsoon.

The high PC2 value composite features a circulation anomaly with less east-west wind across the low-latitude oceanic areas extending from ~15°N to 25°N, 50°E to the West Pacific. The corresponding CAPE anomalies exhibit a wave train, with a strong gradient in the same areas. Although the associated OLR anomalies become zonally elongated and centered on the Bay of Bengal and South China Sea, their distribution does not exhibit east-west propagation (Fig. 10d). The absence of a wave train might be due to the relatively low spatial resolution of the OLR data.

Similar to the low PC1 values, the low PC3 composite exhibits enhanced southwestward atmospheric transport at low levels, greater CAPE over the Arabian Sea and Bay of Bengal, and stronger convection centered over the northern Indian subcontinent (Fig. 11). However, the anomaly pattern differs little. In general, all weather events can include unique attributes that project onto higher EOFs but that are governed by physics similar to those of the signals that generate the leading EOFs (Roundy et al., 2015). In this sense, it is difficult to determine whether the high PC3 value composite is significantly different from the high PC1 value composite.

Based on the three PC composites in Figs. 9-11, large deep convection differences between the composites based on high and low values largely occurred over the northern Bay of Bengal. Therefore, the BL sources of BL-to-TL transport varied across a wide range of spatiotemporal scales. Nevertheless, their sub-seasonal behavior is tied to the strength of the persistent deep convection over the southeastern flank of the TP and its neighboring regions (as shown by the significant anomalies of OLR in Fig 9(f), 10(f), and 11(f)). This region is overlaps well with the pathway in Fig. 8 of Pan et al. (2016), who stated that the southern flank of the Tibetan Plateau is a primary location for BL tracers to be lofted into the UTLS. In fact, based on a similar trajectory model analysis, Bergman et al. (2013) concluded that most air masses in the ASM anticyclone passed through of a fairly narrow uplift transport “conduit”. Therefore, the ASM transport behaves like a 'bubble' during the uplift process from the BL to the TL and is dominated by the stationary, localized uplift over the southeastern flank of the Tibetan Plateau (Vogel et al, 2015, 2016; Pan et al., 2016).

4 Conclusion and remarks

Quantifying the primary BL sources of the BL-to-TL transport and the associated variability is important for better understanding the chemical behavior of the UTLS and the dominant driving processes. The research on this issue plays a vital role in better understanding the variability in the chemical composition of the TL layer over the ASM region and is still generally in the early stages (Vogel et al., 2015; Pan et al., 2016). In this study, we preformed Lagrangian modeling of the atmospheric transport processes in the ASM region during the summer seasons of 2001-2013. Using a 3D labeling and trajectory tracking method, we focused on the sub-seasonal variability in the BL sources. In addition to verifying earlier analyses, the results presented here reveal interesting details and are summarized as follows:

(1) Climatologically, the Tibetan Plateau and India, particularly the southern slope of the Himalayas, are the most impactful BL sources of BL-to-TL transport. These findings differ slightly from those of some previous studies but are complementary to those of others (e.g., Bergman et al., 2013; Pan et al., 2016).

(2) Sub-seasonal-scale BL source variability is notable during the summer season. The different source regions that contribute to the BL-to-TL transport are also highly variable in terms of location and shape during the summer. Our analysis also shows that distinct 10-20-day and 30–60-day low-frequency oscillations exist in both of the key regions from May to July. These findings highlight the role of sub-seasonal variability in the summer monsoon system in the transport of BL air masses to the tropopause over the ASM region.

(3) Although the EOF analysis does not fully describe variations in the BL sources associated with robust physical or spatial patterns, the results indicate that the BL sources varied across a wide range of spatiotemporal scales. The composite analysis shows that the variation in the persistent deep convection concentrated along the southeastern flank of the Tibetan Plateau and over the Bay of Bengal plays a dominant role in the modulation of the sub-seasonal behavior of BL sources.

These results have established a climatology for BL sources associated with BL-to-TL transport during the summer period and can be regarded as an extension of our earlier work (Chen et al.2012). We hope that the results of this study will provide some clarification of the controversial BL sources over the ASM region. Additionally, the sub-seasonal spatiotemporal changes during the summer season have not been quantitatively described in previous studies. A thorough examination of the three-dimensional structure and spatiotemporal patterns of the "conduit" or "chimney" over this region need to be further analyzed to better understand the regional vertical transport. The climatic variability in the BL sources over the ASM region will also be investigated to identify how the BL sources have changed in recent decades and their relationships with global and regional climate change.

Acknowledgments

This research was jointly funded by the Training Program of the Major Research Plan of the National Natural Science Foundation of China (Grant No. 91637102) and the National Natural Science Foundation of China (Grant No. 41475036). We thank the European Centre of Medium-Range Weather Forecasts (ECMWF) for providing the ERA-Interim reanalysis data. The authors are also grateful for the FLEXPART model, which is available at http://flexpart.eu.

References

Bannister, R. N., O'Neill, A., Gregory, A. R., and Nissen, K. M.: The role of the south-east Asian monsoon and other seasonal features in creating the 'tape-recorder' signal in the Unified Model, Q J Roy Meteor Soc, 130, 1531-1554, 10.1256/qj.03.106, 2004.

Bergman, J. W., Fierli, F., Jensen, E. J., Honomichl, S., and Pan, L. L.: Boundary layer sources for the Asian anticyclone: Regional contributions to a vertical conduit, Journal of Geophysical Research: Atmospheres, 118, 2560-2575, 10.1002/jgrd.50142, 2013.

Berthet, G., Esler, J. G., and Haynes, P. H.: A Lagrangian perspective of the tropopause and the ventilation of the lowermost stratosphere, J. Geophys. Res., 112, D18102, 10.1029/2006jd008295, 2007.

Bian, J., Pan, L. L., Paulik, L., Vömel, H., Chen, H., and Lu, D.: In situ water vapor and ozone measurements in Lhasa and Kunming during the Asian summer monsoon, Geophys Res Lett, 39, L19808, 10.1029/2012gl052996, 2012.

Chen, B., Xu, X. D., Yang, S., and Zhao, T. L.: Climatological perspectives of air transport from atmospheric boundary layer to tropopause layer over Asian monsoon regions during boreal summer inferred from Lagrangian approach, Atmos. Chem. Phys., 12, 5827-5839, 10.5194/acp-12-5827-2012, 2012.

Chen, B., and Xiang-De, X. U.: Climatology of wintertime long-distance transport of surface-layer air masses arriving urban Beijing in 2001–2012, Atmospheric Environment, 151, 70-81,2017.

Chen, T.-C., Yen, M.-C., and Weng, S.-P.: Interaction between the Summer Monsoons in East Asia and the South China Sea: Intraseasonal Monsoon Modes, J Atmos Sci, 57, 1373-1392, 10.1175/1520-0469.

Dee, D. P., Uppala, S. M., Simmons, A. J., Berrisford, P., Poli, P., Kobayashi, S., Andrae, U., Balmaseda, M. A., Balsamo, G., Bauer, P., Bechtold, P., Beljaars, A. C. M., van de Berg, L., Bidlot, J., Bormann, N., Delsol, C., Dragani, R., Fuentes, M., Geer, A. J., Haimberger, L., Healy, S. B., Hersbach, H., Hólm, E. V., Isaksen, L., Kållberg, P., Köhler, M., Matricardi, M., McNally, A. P., Monge-Sanz, B. M., Morcrette, J. J., Park, B. K., Peubey, C., de Rosnay, P., Tavolato, C., Thépaut, J. N., and Vitart, F.: The ERA-Interim reanalysis: configuration and performance of the data assimilation system, Q J Roy Meteor Soc, 137, 553-597, 10.1002/qj.828, 2011.

Deng, X. J., Tie, X. X., Zhou, X. J., Wo, D., Zhong, L. J., Tan, H. B., Li, F., Huang, X. Y., Bi, X. Y., and Deng, T.: Effects of Southeast Asia biomass burning on aerosols and ozone concentrations over the Pearl River Delta (PRD) region, Atmospheric Environment, 42, 8493-8501, 10.1016/j.atmosenv.2008.08.013, 2008.

Ding, Y., and Chan, J. C. L.: The East Asian summer monsoon: an overview, Meteorol. Atmos. Phys., 89, 117-142, 10.1007/s00703-005-0125-z, 2005.

Forster, C., Stohl, A., and Seibert, P.: Parameterization of Convective Transport in a Lagrangian Particle Dispersion Model and Its Evaluation, J. Appl. Meteorol. Climatol., 46, 403-422, 10.1175/jam2470.1, 2007.

Forster, P. M. d. F., and Shine, K. P.: Radiative forcing and temperature trends from stratospheric ozone changes, J. Geophys. Res., 102, 10841-10855, 10.1029/96jd03510, 1997.

Fu, R., Hu, Y. L., Wright, J. S., Jiang, J. H., Dickinson, R. E., Chen, M. X., Filipiak, M., Read, W. G., Waters, J. W., and Wu, D. L.: Short circuit of water vapor and polluted air to the global stratosphere by convective transport over the Tibetan Plateau, Proceedings of the National Academy of Sciences of the United States of America, 103, 5664-5669, 10.1073/pnas.0601584103, 2006.

Garny, H., and Randel, W. J.: Transport pathways from the Asian monsoon anticyclone to the stratosphere, Atmos. Chem. Phys., 16, 2703-2718, 10.5194/acp-16-2703-2016, 2016.

Gettelman, A., Hoor, P., Pan, L. L., Randel, W. J., Hegglin, M. I., and Birner, T.: The extratropical upper troposphere and lower stratosphere, Rev Geophys, 49, RG3003, 10.1029/2011rg000355, 2011.

He, J., Ju, J., Wen, Z., Lü, J., and Jin, Q.: A review of recent advances in research on Asian monsoon in China, Adv. Atmos. Sci., 24, 972-992, 10.1007/s00376-007-0972-2, 2007.

Heath, N. K., and Fuelberg, H. E.: Using a WRF simulation to examine regions where convection impacts the Asian summer monsoon anticyclone, Atmos. Chem. Phys., 14, 2055-2070, 10.5194/acp-14-2055-2014, 2014.

Hegglin, M. I., Gettelman, A., Hoor, P., Krichevsky, R., Manney, G. L., Pan, L. L., Son, S. W., Stiller, G., Tilmes, S., Walker, K. A., Eyring, V., Shepherd, T. G., Waugh, D., Akiyoshi, H., Añel, J. A., Austin, J., Baumgaertner, A., Bekki, S., Braesicke, P., Brühl, C., Butchart, N., Chipperfield, M., Dameris, M., Dhomse, S., Frith, S., Garny, H., Hardiman, S. C., Jöckel, P., Kinnison, D. E., Lamarque, J. F., Mancini, E., Michou, M., Morgenstern, O., Nakamura, T., Olivié, D., Pawson, S., Pitari, G., Plummer, D. A., Pyle, J. A., Rozanov, E., Scinocca, J. F., Shibata, K., Smale, D., Teyssèdre, H., Tian, W., and Yamashita, Y.: Multimodel assessment of the upper troposphere and lower stratosphere: Extratropics, J. Geophys. Res., 115, D00M09, 10.1029/2010jd013884, 2010.

Hoor, P., Wernli, H., Hegglin, M. I., and Bönisch, H.: Transport timescales and tracer properties in the extratropical UTLS, Atmos. Chem. Phys., 10, 7929-7944, 10.5194/acp-10-7929-2010, 2010.

James, R., Bonazzola, M., Legras, B., Surbled, K., and Fueglistaler, S.: Water vapor transport and dehydration above convective outflow during Asian monsoon, Geophys Res Lett, 35, L20810, 10.1029/2008gl035441, 2008.

Li, D., Vogel, B., Bian, J., Müller, R., Pan, L. L., Günther, G., Bai, Z., Li, Q., Zhang, J., Fan, Q., and Vömel, H.: Impact of typhoons on the composition of the upper troposphere within the Asian summer monsoon anticyclone: the SWOP campaign in Lhasa 2013, Atmos. Chem. Phys. Discuss., 2016, 1-27, 10.5194/acp-2016-875, 2016.

Li, Q., Jiang, J. H., Wu, D. L., Read, W. G., Livesey, N. J., Waters, J. W., Zhang, Y., Wang, B., Filipiak, M. J., Davis, C. P., Turquety, S., Wu, S., Park, R. J., Yantosca, R. M., and Jacob, D. J.: Convective outflow of South Asian pollution: A global CTM simulation compared with EOS MLS observations, Geophys Res Lett, 32, L14826, 10.1029/2005gl022762, 2005.

Liebmann, B.: Description of a complete (interpolated) outgoing longwave radiation dataset, Bull. Amer. Meteor. Soc., 77, 1275-1277, 1996.

Müller, S., Hoor, P., Bozem, H., Gute, E., Vogel, B., Zahn, A., Bönisch, H., Keber, T., Krämer, M., Rolf, C., Riese, M., Schlager, H., and Engel, A.: Impact of the Asian monsoon on the extratropical lower stratosphere: trace gas observations during TACTS over Europe 2012, Atmos. Chem. Phys., 16, 10573-10589, 10.5194/acp-16-10573-2016, 2016.

Madden, R. A., and Julian, P. R.: Observations of the 40–50-Day Tropical Oscillation—A Review, Mon Weather Rev, 122, 814-837, 10.1175/1520-0493(1994)122<0814:ootdto>2.0.co;2, 1994.

Nützel, M., Dameris, M., and Garny, H.: Movement, drivers and bimodality of the South Asian High, Atmos. Chem. Phys., 16, 14755-14774, 10.5194/acp-16-14755-2016, 2016.

Orbe, C., Waugh, D. W., and Newman, P. A.: Air-mass origin in the tropical lower stratosphere: The influence of Asian boundary layer air, Geophys Res Lett, 42, 4240-4248, 10.1002/2015gl063937, 2015.

Pan, L. L., Honomichl, S. B., Kinnison, D. E., Abalos, M., Randel, W. J., Bergman, J. W., and Bian, J.: Transport of Chemical Tracers from the Boundary Layer to Stratosphere Associated with the Dynamics of the Asian Summer Monsoon, Journal of Geophysical Research: Atmospheres, n/a-n/a, 10.1002/2016jd025616, 2016.

Park, M., Randel, W. J., Emmons, L. K., Bernath, P. F., Walker, K. A., and Boone, C. D.: Chemical isolation in the Asian monsoon anticyclone observed in Atmospheric Chemistry Experiment (ACE-FTS) data, Atmos. Chem. Phys., 8, 757-764, 2008.

Park, M., Randel, W. J., Emmons, L. K., and Livesey, N. J.: Transport pathways of carbon monoxide in the Asian summer monsoon diagnosed from Model of Ozone and Related Tracers (MOZART), J. Geophys. Res., 114, D08303, 10.1029/2008jd010621, 2009.

Randel, W. J., and Park, M.: Deep convective influence on the Asian summer monsoon anticyclone and associated tracer variability observed with Atmospheric Infrared Sounder (AIRS), Journal of Geophysical Research: Atmospheres, 111, D12314, 10.1029/2005jd006490, 2006.

Randel, W. J., Park, M., Emmons, L., Kinnison, D., Bernath, P., Walker, K., Boone, C., and Pumphrey, H.: Asian monsoon transport of pollution to the stratosphere, Science, 328, 611-613, 2010.

Randel, W. J., Pan, L. L., and Bian, J.: Workshop on Dynamics, Transport and Chemistry of the UTLS Asian Monsoon, Adv. Atmos. Sci., 33, 1096-1098, 2016.

Rauthe-Schöch, A., Baker, A. K., Schuck, T. J., Brenninkmeijer, C. A. M., Zahn, A., Hermann, M., Stratmann, G., Ziereis, H., van Velthoven, P. F. J., and Lelieveld, J.:

Atmos. Chem. Phys. Discuss., doi:10.5194/acp-2017-216, 2017
Manuscript under review for journal Atmos. Chem. Phys.
Discussion started: 27 March 2017

Trapping, chemistry, and export of trace gases in the South Asian summer monsoon observed during CARIBIC flights in 2008, Atmos. Chem. Phys., 16, 3609-3629, 10.5194/acp-16-3609-2016, 2016.

Scheeren, H. A., Lelieveld, J., Roelofs, G. J., Williams, J., Fischer, H., de Reus, M., de Gouw, J. A., Warneke, C., Holzinger, R., Schlager, H., Klupfel, T., Bolder, M., van der Veen, C., and Lawrence, M.: The impact of monsoon outflow from India and Southeast Asia in the upper troposphere over the eastern Mediterranean, Atmos Chem Phys, 3, 1589-1608, 2003.

Solomon, S., Rosenlof, K. H., Portmann, R. W., Daniel, J. S., Davis, S. M., Sanford, T. J., and Plattner, G.-K.: Contributions of Stratospheric Water Vapor to Decadal Changes in the Rate of Global Warming, Science, 327, 1219-1223, 10.1126/science.1182488, 2010.

Stohl, A., and Seibert, P.: Accuracy of trajectories as determined from the conservation of meteorological tracers, Q J Roy Meteor Soc, 124, 1465-1484, 10.1002/qj.49712454907, 1998.

Stohl, A., Forster, C., Frank, A., Seibert, P., and Wotawa, G.: Technical note: The Lagrangian particle dispersion model FLEXPART version 6.2, Atmos Chem Phys, 5, 2461-2474, 2005.

Sugimoto, S., and Ueno, K.: Formation of mesoscale convective systems over the eastern Tibetan Plateau affected by plateau-scale heating contrasts, J. Geophys. Res., 115, D16105, 10.1029/2009jd013609, 2010.

Vincent, D. G., Fink, A., Schrage, J. M., and Speth, P.: High- and Low-Frequency Intraseasonal Variance of OLR on Annual and ENSO Timescales, J Climate, 11, 968-986, 10.1175/1520-0442(1998)011<0968:halfiv>2.0.co;2, 1998.

Vogel, B., Günther, G., Müller, R., Grooß, J. U., Hoor, P., Krämer, M., Müller, S., Zahn, A., and Riese, M.: Fast transport from Southeast Asia boundary layer sources to northern Europe: rapid uplift in typhoons and eastward eddy shedding of the Asian monsoon anticyclone, Atmos. Chem. Phys., 14, 12745-12762, 10.5194/acp-14-12745-2014, 2014.

Vogel, B., Günther, G., Müller, R., Grooß, J. U., and Riese, M.: Impact of different Asian source regions on the composition of the Asian monsoon anticyclone and of the extratropical lowermost stratosphere, Atmos. Chem. Phys., 15, 13699-13716, 10.5194/acp-15-13699-2015, 2015.

Vogel, B., Günther, G., Müller, R., Grooß, J. U., Afchine, A., Bozem, H., Hoor, P., Krämer, M., Müller, S., Riese, M., Rolf, C., Spelten, N., Stiller, G. P., Ungermann, J., and Zahn, A.: Long-range transport pathways of tropospheric source gases originating in Asia into the northern lower stratosphere during the Asian monsoon season 2012, Atmos. Chem. Phys. Discuss., 2016, 1-40, 10.5194/acp-2016-463, 2016.

Vogelezang, D. H. P., and Holtslag, A. A. M.: Evaluation and model impacts of alternative boundary-layer height formulations, Bound-Lay Meteorol, 81, 245-269, 10.1007/bf02430331, 1996.

Wernli, H., and Bourqui, M.: A Lagrangian "1-year climatology" of (deep) cross-tropopause exchange in the extratropical Northern Hemisphere, J. Geophys. Res., 107, 4021, 10.1029/2001jd000812, 2002.

Wright, J. S., Fu, R., Fueglistaler, S., Liu, Y. S., and Zhang, Y.: The influence of summertime convection over Southeast Asia on water vapor in the tropical stratosphere, Journal of Geophysical Research: Atmospheres, 116, D12302, 10.1029/2010jd015416, 2011.

Wu, G., and Zhang, Y.: Tibetan Plateau Forcing and the Timing of the Monsoon Onset over South Asia and the South China Sea, Mon Weather Rev, 126, 913-927, 10.1175/1520-0493(1998)126<0913:tpfatt>2.0.co;2, 1998.

Yan, R., and Bian, J.: Tracing the boundary layer sources of carbon monoxide in the Asian summer monsoon anticyclone using WRF-Chem, Adv. Atmos. Sci., 32, 943-951, 10.1007/s00376-014-4130-3, 2015.

Yanai, M., and Li, C.: Mechanism of Heating and the Boundary Layer over the Tibetan Plateau, Mon Weather Rev, 122, 305-323, 10.1175/1520-0493(1994)122<0305:mohatb>2.0.co;2, 1994.

Zhang, Q., Wu, G., and Qian, Y.: The Bimodality of the 100 hPa South Asia High and its Relationship to the Climate Anomaly over East Asia in Summer, Journal of the Meteorological Society of Japan. Ser. II, 80, 733-744, 10.2151/jmsj.80.733, 2002.

Atmos. Chem. Phys. Discuss., doi:10.5194/acp-2017-216, 2017
Manuscript under review for journal Atmos. Chem. Phys.
Discussion started: 27 March 2017

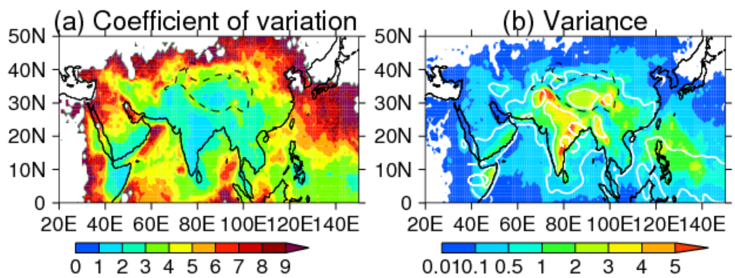

Figure 1: (a) The coefficient of variation (CV) and (b) variance for BL-to-TL sources (represented by the number of total trajectories) in each 1° × 1° longitude-latitude grid cell. Both are calculated from daily time series.

Atmos. Chem. Phys. Discuss., doi:10.5194/acp-2017-216, 2017
Manuscript under review for journal Atmos. Chem. Phys.
Discussion started: 27 March 2017

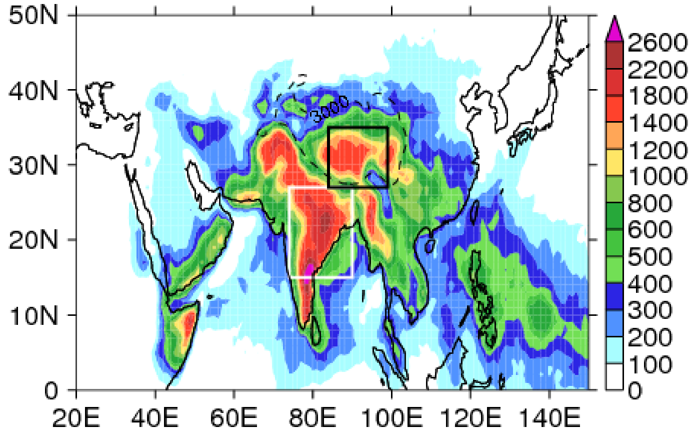

Figure 2: Seasonal density field of all the BL-to-TL trajectories within the boundary layer in 1° × 1° longitude-latitude bins averaged over the summer period (May-July) for 2001–2013. BL-to-TL trajectories are defined as trajectories departing the BL and crossing the tropopause along their journey. Black dashed lines represent the 3000 m elevation contour. The two boxes indicate the selected regions for the Tibetan Plateau (black) and the Indian continent (white).

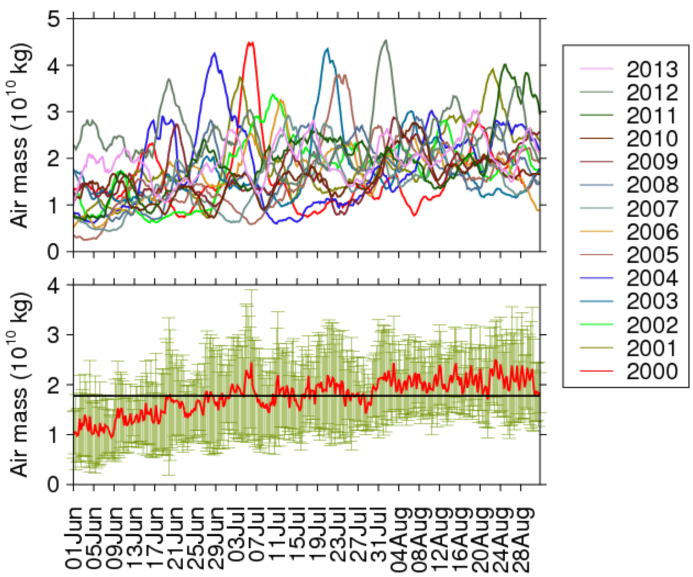

Figure 3: (Top) Daily evolution of the total air masses of BL-to-TL uplift associated with the ASM anticyclone for each year from 2000-2013 (with a nine-point moving average). The total air mass is calculated by counting the number of tropopause-crossing trajectories and multiplying by the associated mass. (Bottom) The 2000-2013 average. The error bars in the bottom panel represent the standard deviation ($\pm\sigma$).

Atmos. Chem. Phys. Discuss., doi:10.5194/acp-2017-216, 2017
Manuscript under review for journal Atmos. Chem. Phys.
Discussion started: 27 March 2017

Atmospheric Chemistry and Physics
Open Access
Discussions

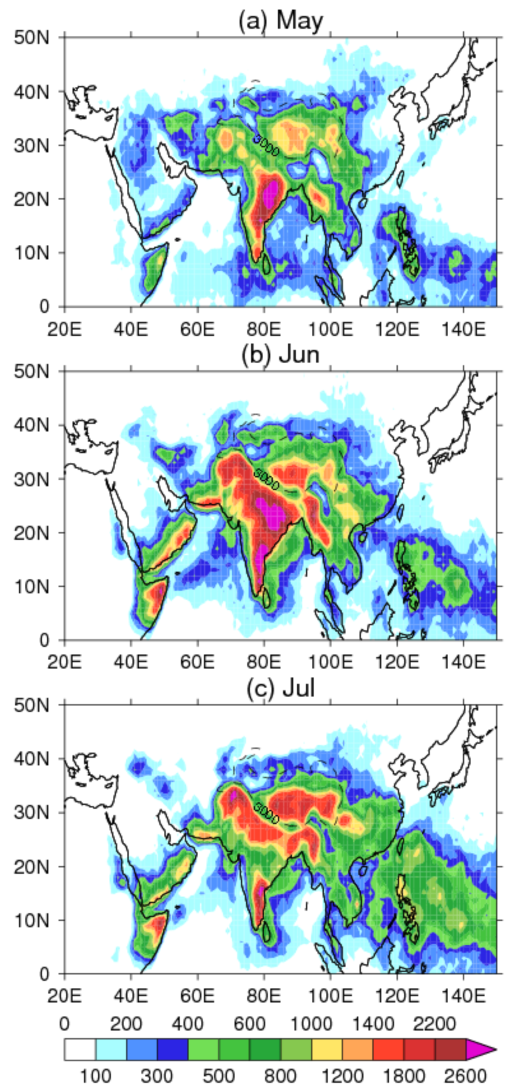

Figure 4: Same as Figure. 2 but for May, June and July.

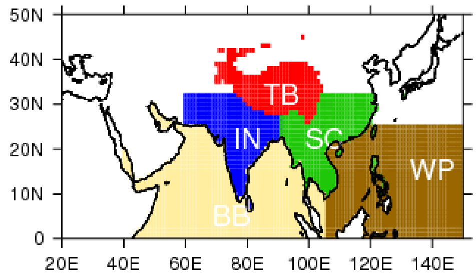

Figure 5: Domains and the abbreviations of the regions of interest. TB represents the Tibetan Plateau region with elevations higher than 2500 m; SC represents southern China, including a large part of the Indochinese Peninsula; IN indicates the Indian subcontinent and part of the southern slope of the Himalayas; BB represents the Bay of Bengal and the Arabian Sea; and WP represents the western Pacific, including the South China Sea and the Sea of Japan.

Atmos. Chem. Phys. Discuss., doi:10.5194/acp-2017-216, 2017
Manuscript under review for journal Atmos. Chem. Phys.
Discussion started: 27 March 2017

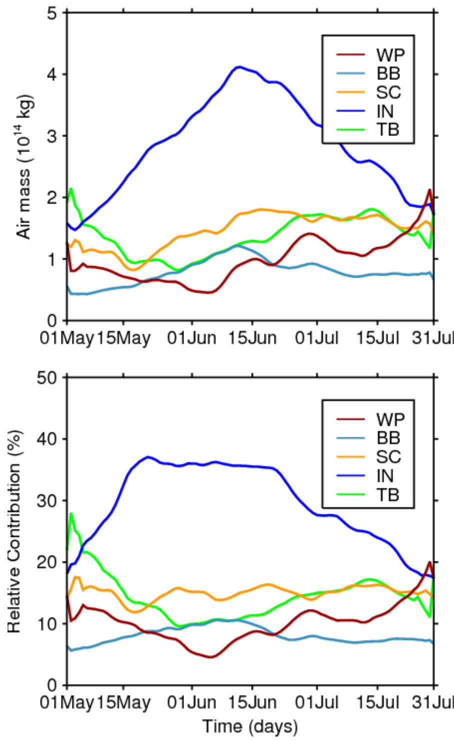

Figure 6: (Top) The daily variation in the multi-year (2001-2013) mean air masses uplifted by BL-to-TL trajectories in the five different regions (scale multiplied by a factor of 10^{14}) from May 1 to 31 July. (Bottom) The corresponding relative contributions to the total air mass. Both graphs take into account the area of each source region. The abbreviations represent the five regions listed in Figure. 5.

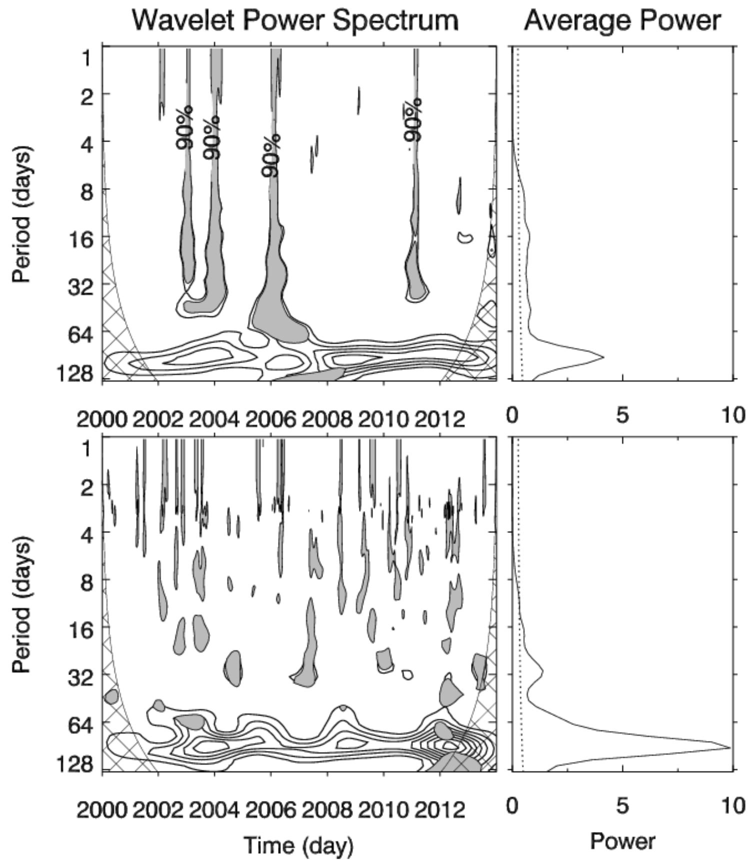

Figure 7: (Left panels) The local normalized wavelet power spectrum derived from the daily series of BL area-averaged sources for (top) TP (25°–35°N, 85°–95°E) and (bottom) IN (15°–25°N, 75°–85°E). The TP and IN regions are shown as boxes in Fig. 2. (Right panels) The corresponding averaged spectrum power. In the left panels, the shaded areas are significant at the 90% confidence level. In the right panels, the solid lines represent the wavelet spectrum, and the dashed lines are the 95% confidence curves. Note that the Morlet wavelet analysis is based on the multi-year data set.

Atmospheric Chemistry and Physics
Open Access
Discussions

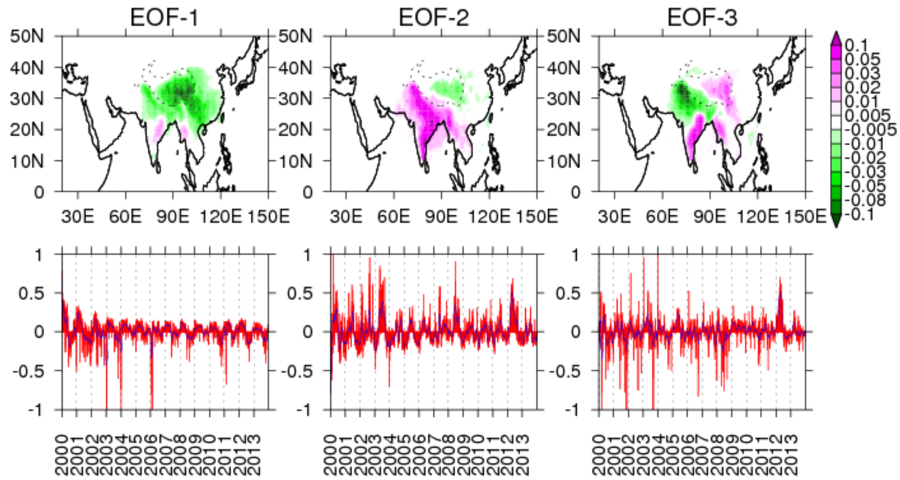

Figure 8: (Top) The three leading EOFs (EOF-1 explains 14.6% of the variance; EOF-2 explains 12.7%; and EOF-3 explains 9.8%) of the anomalies of daily BL sources during May–July computed for the ASH region. (Bottom) The corresponding time weight coefficient for each EOF.

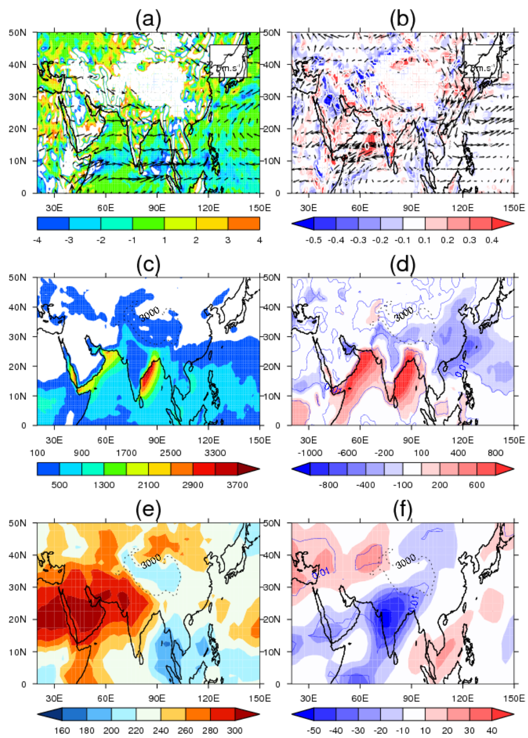

Figure 9: High-value composite maps constructed from the 50 highest positive PC1 values for (a) low-level winds fields (vector) and the vertical velocity (color, pa·s^{-1}) at 850 hPa, (c) convective available potential energy (CAPE, J·kg^{-1}), and (e) outgoing longwave radiation (OLR, K). All meteorological fields are based on ERA-Interim reanalysis data, excepting for the OLR, which is from NOAA polar-orbiting satellites. (b), (d), and (f) are the corresponding differences between the composites of 50 highest and lowest PC1 values (blue indicates negative and red indicates positive). Only significant anomalies at the 90% confidence level according to Student's t-test are contoured.

Atmos. Chem. Phys. Discuss., doi:10.5194/acp-2017-216, 2017
Manuscript under review for journal Atmos. Chem. Phys.
Discussion started: 27 March 2017

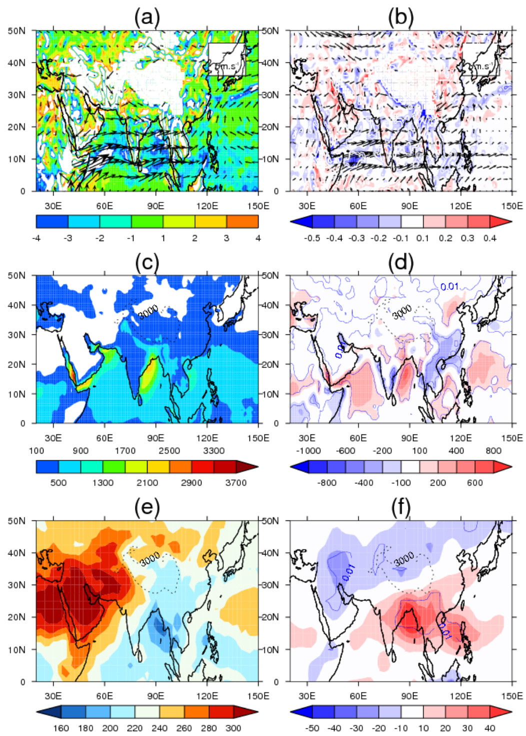

Figure 10: Same as Figure. 9 but for PC2.

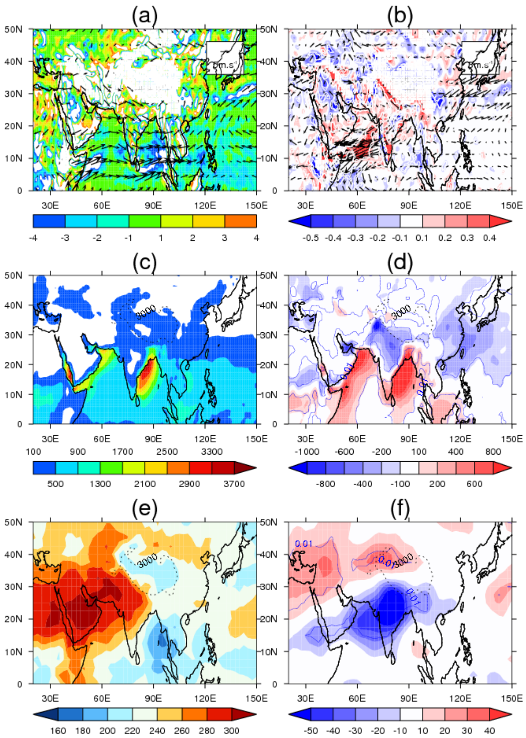

Figure 11: Same as Figure. 9 but for PC3.